ORIGINAL RESEARCH PAPER

Anatomy

CAN CLEOME VISCOSA PROTECT AGAINST DIABETIC SCIATIC NEUROPATHY IN ALBINO RATS? A HISTOLOGICAL STUDY

KEY WORDS: neuropathy - streptozotocin - Diabetes - Cleome viscosa- - antioxidants.

Mohamed E.A. Mostafa Ph.D., Professor, Anatomy Dept., Faculty of Medicine, University of Tabuk & Cairo.

Abdullah H. Altemani Ph.D., Assistant Professor, Family and Community medicine Dept., Faculty of Medicine, University of Tabuk, Saudi Arabia.

Ashraf M. F. Kamel* Ph.D., Professor, Preparatory Health Sciences Dept., Riyadh Colleges of Dentistry and Pharmacy. *Corresponding Author

ABSTRACT

Background: The possible protective role of Cleome Viscosa (Cl V) in experimental peripheral neuropathy was investigated in diabetic (streptozotocin [STZ] induced) Albino rats.

Material and Methods: Forty adult male albino rats were divided into four groups; control, sham control, experimental group that received STZ and a protection group that received Cl V 4 weeks before STZ. Sciatic nerve specimens were subjected to light and electron microscopy as well as morphometric analysis.

Results: The sciatic nerve in diabetic rats showed axonal shrinkage, axon–myelin separation, onion-bulb, vacuolization of the myelin sheath with formation of fermentation chambers, thickening of the epineurium, as well as sub-epineurial edema. Administration of Cl V prior to induction of diabetes was associated with decreased DPN histopathological abnormalities.

Conclusion: Cl V administration minimized the histological manifestations of STZ induced DPN.

Introduction

Diabetes mellitus (DM) is one of the most common metabolic disorders. Type 2 diabetes mellitus (T2DM) accounts for more than 90% of cases of diabetes. According to the International Diabetes Federation (IDF) atlas 2013, there are 381.8 million diabetic patients aged 20–79 years, and this is expected to increase by 55% to reach 591.9 million by the year 2035 (**Guariguata, 2014)**. In Saudi Arabia, DM is the most prevalent chronic disease. It is estimated to be around 34.1% in males and 27.6% in females (**Alqurashi** et al., 2011). It is the top frequent disease (10.5%) in hospitalized patients in Saudi Arabia (Alamoudi et al., 2009).

Diabetic peripheral neuropathy (DPN) is one of the most common chronic complications of diabetes mellitus and often presents as a distal, symmetric, sensori-motor neuropathy (Farmer et al., 2012) with manifestations of autonomic dysfunction (Tesfaye & Selvarajah, 2012), and can lead to leg ulcers, limb amputation, and even death (Ewing et al., 1976; Vileikyte et al., 2003). However, the pathogenesis of DPN has not been fully clarified. It is accepted that multiple factors related to chronic uncontrolled hyperglycemia contribute to the development of DPN, including the polyol pathway, advanced glycation end-product formation, and activation of protein kinase C, and so on (**Yasuda *et al.*, 2003; Chan et al., 2011)**.

Oxidative stress appears to be the most important pathogenic factor underlying diabetic complications including neuropathy. Lower endogeneous antioxidants and elevated lipid peroxidation levels are risk factors for the development of macrovascular and microvascular diabetic complications such as retinopathy, neuropathy, nephropathy, and atherosclerosis **(Fox et al., 2004)**. Mechanisms that contribute to increased oxidative stress in DM may include not only increased nonenzymatic glycosylation but also changes in the status of antioxidant defense systems, resulting in the development of complications and localized tissue damage **(Gürpinar et al., 2012)**. As oxidative stress is the main cause of diabetic complications, administration of antioxidants appears to be one of the most reasonable therapeutic approaches. Some studies showed that diabetic complications may be reduced by antioxidant therapies, including supplementation with vitamins C and E, alpha lipoic acid, and l-carnitine, in a variety of experimental animal models of DM **(Kawada et al., 2012)**.

Recent evidence demonstrates that inflammation is closely related to diabetes and its complications **(Das and Mukhopadhyay, 2011; Golbidi et al., 2011)**. Therefore, introducing moderate anti-inflammatory therapy may have an effect on DPN. However, nonsteroidal anti-inflammatory drugs (NSAIDs) have limited clinical application due to toxic side effects (**Agrawal & Kant, 2014)**. Thus, it is extremely important to explore new, safe, and effective anti-inflammatory therapeutic drugs.

Cleome viscosa (CL V) is a widely distributed herb throughout northern and southern Hijaz, Saudi Arabia, especially in Tabuk and is known as Om-Hanif. Traditionally, this plant is used to treat diarrhea, fever, inflammation, liver diseases, bronchitis, skin diseases, and malarial fever. Its juice is useful in piles, lumbago and earache **(Jana and Biswas, 2011)**. The plant is rich in lignans, flavonoids, saponins, ascorbic acid, and polyunsaturated fatty acid. Its extract has antipyretic, hepatoprotective, anti-helminthic, analgesic, anti-inflammatory, antioxidant, immunomodulatory, antimalarial and anti-diarrheal activities **(Bose et al., 2011)**.

Although some studies have cited the antidiabetic effect of CL V (**Boyina Chaya and Chakrapani, 2015)**, there are few studies on its potential effect in the prevention of DPN.

Aim of the work

The aim of the present work is to study the histological changes in the sciatic nerve of rats after experimental induction of diabetes mellitus.

It is also aimed to detect the possible protective effect of CL V when given prior to the induction of diabetes.

Moreover, morphometric quantification of the cross-sectional area and the total number (and percentage) of myelinated axons, (both the normally and abnormally appearing) in the entire sciatic nerve, among the different groups will be done, then the obtained data will be analyzed statistically.

Material and Methods

Drugs and chemicals:

-Streptozotocin was purchased from (Sigma Chemical Company, St. Louis, MO, USA
) .

- Cleome Viscosa (*Cl V)* plant will be collected from various parts of Tabuk region, Kingdom of Saudi Arabia (KSA) in the month of September 2016. They will be authenticated and processed in the College of Pharmacy, Riyadh Colleges of Dentistry and Pharmacy, Riyadh, KSA. The selected parts of the plants will be dried in the

shade at a temperature ranging from 21 to 30°C for 15-30 days. Afterwards, the selected plant parts will be chopped and grounded. They will be extracted with ethanol in a Soxhlet apparatus. The ethanolic extract will be distilled, evaporated, and dried under vacuum. The Cleome viscosa (*Cl V*) extracts will be freshly prepared as 400 mg/kg doses, dissolved in 1ml ethanol and administered (once daily, orally by gastric gavage) for 4 weeks before streptozotocin administration **(Boddapati et al., 2014)**.

- All other chemicals were of analytical grade.

Animals

This study was carried out on 40 adult male albino rats, aged between 20–24weeks and weighing 195-255 ± 15 g (mean ± SD, 225 ± 3.23) at the beginning of the experiment. The study was conducted at the Animal House of Kasr-Al-Aini, Faculty of Medicine, Cairo University, according to the Ethical Guidelines for the Care and Use of Laboratory Animals. All experimental animal procedures were conformed to the principles laid down by the National Research Council Guide for the Care and Use of Laboratory Animals with CU-IACUC reviewers approval number CUIIIS1416.

The use of the rats in the current work was justified by the established similarity of peripheral nerves in rats to those of human as regards morphology, nerve conduction velocities, blood flow, as well as the biochemical abnormalities **(Kawada, et al., 2012).**

Experimental design:

The animals were divided into the following groups:

Group I (control group): eight rats received no treatment.
Group II (sham control vehicle group): sixteen rats that were subdivided into 2 equal subgroups:

- Subgroup IIa (sham control ethanol-treated group): received 1ml ethanol daily (by gastric gavage) for 7 weeks.
- Subgroup IIb (sham control citric *acid buffer*-treated group): received an intraperitoneal single dose of 1ml citric acid buffer (pH 4.5) four weeks after onset of the experiment.

Group III (*diabetic untreated group*): eight diabetic rats. Diabetes was induced by streptozotocin, four weeks after the onset of the experiment (**Chen et al., 2016)**.

Group IV (*diabetic group treated with Cl V*): eight diabetic rats. They received a daily single dose of 400 mg/kg Cl V dissolved in 1ml ethanol and administered (by gastric gavage) for 7 weeks. Administration of *CL V* started 4 weeks before development of diabetes.

Induction of diabetes:

Diabetes was induced in 16 rats (groups III & IV) by a single intraperitoneal (IP) injection of streptozotocin (STZ) at a dose of 60 mg/kg dissolved in 1ml citric acid buffer (pH 4.5). Forty-eight hours after STZ injection, development of DM was confirmed by measuring the blood glucose levels in blood samples taken from the retro-orbital veins. Rats with blood glucose levels higher than 200 mg/dl were considered diabetic (**Wu and Huan, 2008)**. Streptozotocin (STZ) has been regarded as the agent of choice for the induction of DM in animals. Being cytotoxic to pancreatic -cells, it can be conveniently used to induce experimental DM in rats (**Lenzen, 2008)**. It was established that a single dose of 60 mg STZ /kg is the best dose to induce diabetes (**Wu and Huan, 2008)**.

Methods:

Body weight measurement:

The body weight of each rat was recorded at the beginning of the experiment and then at the end of the study period for all groups.

Laboratory investigations:

Random blood sugar was measured for all groups. It was done in the Biochemistry Department, Faculty of Medicine, Cairo University. Forty-eight hours after STZ injection, development of DM was confirmed by measuring blood glucose levels in blood samples taken from the retro-orbital veins. Rats with blood glucose levels higher than 200 mg/dl (**Callaghan et al., 2012)** were considered diabetic (normal blood glucose<150 mg/dl).

Light and electron microscopic studies:

Twenty four hours after the last dose of Cl V, animals were anesthetized with pentobarbital sodium (55 mg/kg, IP) and perfused transcardiac (through a puncture at the apex of the left ventricle and a cannula inserted in the aorta) with a 150 ml fixative containing 2.5% paraformaldehyde and 2% glutaraldehyde in 0.1 M phosphate buffer, pH 7.4 at room temperature **(Kissin et al., 2007).** Perfusion continued until both the upper and lower limbs of the rat became stiff. From each animal, both sciatic nerves were dissected out, and stored in the same fixative overnight at 4°C. On the following day, post-fixing in 1% osmium tetroxide for 1 hour, dehydrating through a graded alcohol series, and and embedded in epoxy resin. For light microscopy, serial semithin 1 µm sections were cut using a Zeiss 6M ultramicrotome (Carl Zeiss AG, Germany, Oberkochen and Munich), stained with 1% toluidine blue, and examined. For electron microscopy, ultrathin sections (0.1 µm thick) were collected on copper grids and contrast-stained with uranyl acetate and lead citrate (**Hayat, 2000)**. The sections were examined by JEM-1400A transmission electron microscope (JEOL, Tokyo, Japan) operated at 80 kV at the Faculty of Agriculture Research Park, Cairo University.

Quantitative morphometric analysis:

The measurements were obtained using Leica Qwin 500 image analyzer computer system (England). Analysis was done for the semi thin sections in the different groups according to the method described in a previous study (**Inserra et al., 2000)**. The nerve cross-sectional area (in square micrometers) was determined by manually outlining a digitized image of the nerve at x40 magnification. The calibrated image analysis program calculated the area of the outline.

In each nerve section, the normally appearing myelinated axons were counted at x1000 magnification within 10 randomly selected areas, each of a known area of 1311.8 μm^2 marked by a standard measuring frame and a mean value ± standard deviation (±S.D.) is obtained. Counts were performed by manually marking each normally appearing myelinated axon in succession. The normally appearing myelinated axon count for the entire nerve was then calculated by multiplying the mean axon count per counted area by the nerve cross-sectional area and dividing the product by 1311.8 μm^2.

$$\frac{\text{Mean axon count in the counting area} \times \text{Nerve cross-sectional area}}{\text{Counting area}}$$

The same procedure was repeated to count the abnormally appearing myelinated axons in each nerve section. A percentage is calculated of the normally appearing to the abnormally appearing myelinated axons for each nerve section and the results were plotted graphically.

Statistical Analysis:

The cross-sectional areas, the total number of axons, number (and percentage) of normally appearing myelinated axons and the number (and percentage) of abnormally appearing myelinated axons in the entire sciatic nerve among the different groups will be presented as mean ±S.D.

Statistical analysis will be performed using analysis of variance (ANOVA) followed by post-hoc Tukey HSD test to compare variables among different groups. A value of P< 0.05 will be considered significant (**Armitage and Berry, 1994)**.

Results

Body weight measurements

At baseline, no significant differences in body weight were detected between any of the study groups. A significant decrease in body weight was recorded in STZ-treated animals (P<0.05) when compared with the control group. After treatment with *Cl V*

for 6 weeks, there was no statistically significant difference in body weight compared with the non-treated diabetic group (Table 1, Fig. 1).

Table 1: Body weight (g) measurements (± SD) in the different groups

	Initial values (g. body weight ± SD)	Duration (in weeks)	Final values (g. body weight ± SD)
Control group	250.0 ± 7.1	7	269.2 ± 9.8
Sham control groups	247.2 ± 6.5	7	265.9 ± 8.1
Diabetic group	248.3 ± 6.7	7	202.4 ± 7.5*
Diabetic CL V treated group	239.5 ± 6.9	7	238.7 ± 8.7

* Significantly different from the corresponding value of the control group at P<0.05.

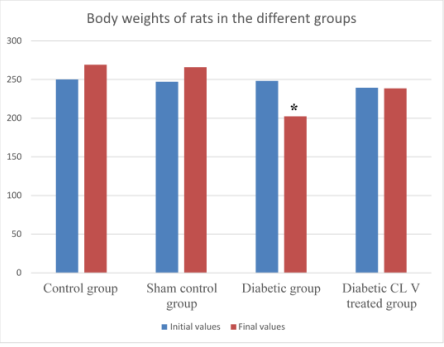

Fig. 1: Body weights of rats in the different groups
* Significantly different from the corresponding value of the control group at P<0.05.

Blood glucose:
Treatment of rats with STZ resulted in a significant increase in serum glucose level when compared with the control values (*P*<0.05) and it remained elevated 6 weeks after STZ. After treatment with *Cl V,* the blood glucose level showed a significant decrease (P<0.05) compared with the non-treated diabetic group (Table 2, Fig. 2).

Table2: Blood glucose (mg/dl) measurements (± SD) in the different groups

	Initial values (mg/dl ± SD)	Duration (in weeks)	Final values (mg/dl ± SD)
Control group	71.9 ± 7.1	7	73.2 ± 9.8
Sham control group	72.1 ± 7.4	7	72.8 ± 9.1
Diabetic group	78.6 ± 6.7	7	355.4 ± 7.1*
Diabetic CL V treated group	77.5 ± 6.9	7	231.4 ± 8.7**

*Significantly different from the corresponding value of the control group at *P*<0.05.
**Significantly different from the corresponding value of the diabetic group at *P*<0.05.

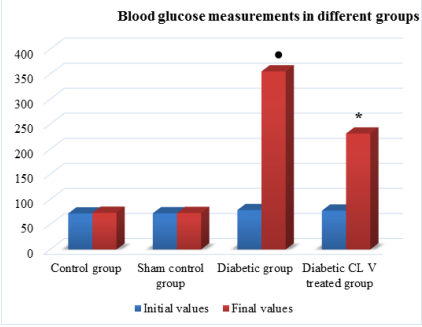

Fig. 2: Blood glucose measurements in the different groups
• Significant compared to diabetic non treated group (P<0.05)
** Significant compared to diabetic non treated group (P<0.05)*

Light Microscopy of Semithin Sections stained with Toluidine blue:
Examination of semithin sections of sciatic nerve sections from rats of the control group showed the normal histological architecture of nerve fascicles containing myelinated and unmyelinated fibers. Variation was detected in the diameter of the nerve fibers. Nerve fibers were grouped in fasciculi, each of which was surrounded by perineurium, and the whole nerve was surrounded by the epineurium. Axons appeared clear with a dark ring of myelin around them (Fig. 3).

Fig. 3: A photomicrograph of a semithin section of the sciatic nerve of a control rat showing intact, compactly arranged nerve fibers of different diameters. The nerve fibers are mainly myelinated with some unmyelinated (Um) fibers in-between. The nerve bundle is surrounded by perineurium (P) of moderate thickness and the entire nerve is enclosed by epineurium (E). **(Toluidine blue X 1000)**

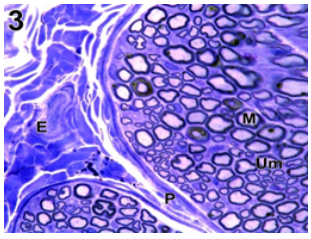

Examination of semithin sections of sciatic nerves in the diabetic group revealed marked changes in the majority of the nerve fibers ranging from axonal atrophy to total axonal destruction and loss. Axonal shrinkage and axon–myelin separation were noted. Onion-bulb formation with layers of Schwann cell processes enwrapping the axon was evident. Changes in the myelin sheath revealed vacuolization of the myelin sheath with formation of fermentation chambers. Marked apparent thickening and irregularity of the epineurium, as well as the presence of sub-epineurial edema were detected (Fig. 4).

Fig. 4: A photomicrograph of a semithin section of the sciatic nerve of a diabetic rat (group III) showing marked changes in the majority of the nerve fibers. Few fibers exhibit axonal retraction (wavy arrow) and periaxonal edema (O). Other fibers present with fermentation chambers (asterisks) Onion-bulb formation (B) of some axons is observed. Severe myelin degeneration described as 'honeycomb' degeneration is also detected (H). The nerve bundle is surrounded by thickened epineurium (E) with sub-epineurial edema (So). **(Toluidine blue X 1000).**

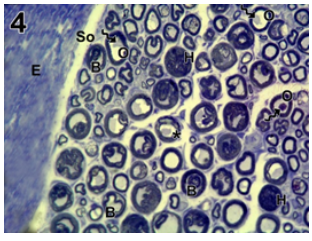

Examination of semithin sections of sciatic nerves in the *Cl V*-treated group revealed apparent improvement in the histological picture as compared to that of diabetic rats. Nerve fibers exhibited a regular outline. These were mainly myelinated. Axonal changes and vacuolization of myelin were less observed. Otherwise, some scattered fibers exhibited an onion bulb appearance. Few regenerating fibers were also seen (Fig. 5).

Fig. 5: A photomicrograph of a semithin section of the sciatic nerve of a diabetic rat treated with Cl V (group IV) showing nerve fibers with a regular outline. These are mainly myelinated (M). Axonal changes and vacuolization of myelin are less obvious.

Otherwise, some fibers appear with onion bulb appearance (B). Few regenerating fibers (R) are observed. (Toluidine blue X 1000)

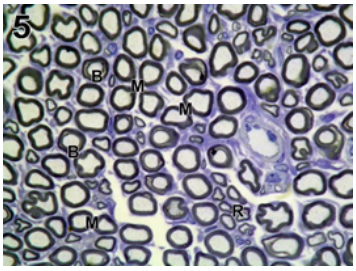

Transmission Electron Microscopy (T.E.M.) results:

Ultrathin sections of sciatic nerve from the control group revealed intact, compactly arranged nerve fibers of different diameters enclosed by the epineurium. The nerve fibers were mainly myelinated with some unmyelinated fibers in-between. The myelin sheath appeared as compact electron-dense material. The axoplasm contained neurotubules and neurofilaments. Schwann cells enclosed the myelinated axons. (Fig. 6).

Fig. 6: An electron micrograph of the sciatic nerve of a control rat showing intact, compactly arranged nerve fibers of different diameters. The nerve fibers were mainly myelinated with some unmyelinated (Um) fibers in-between. The myelin sheath (My) appears as compact electron-dense material. The axoplasm contains neurotubules and neurofilaments (NF). A Schwann cell (S) is seen enclosing a myelinated axon. The nerve is enclosed by epineurium (E). **(TEM X 3000)**

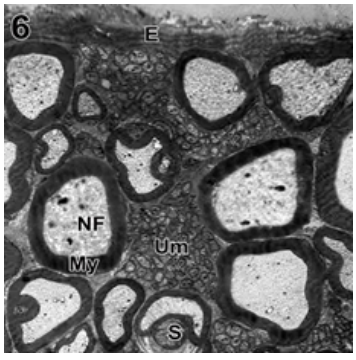

Examination of ultrathin nerve sections of the diabetic group demonstrated demyelination in the majority of myelinated nerve fibers in the form of splitting and decompaction of myelin sheath lamellae, with the formation of fermentation chambers (Fig. 7).

Fig. 7: An electron micrograph of the sciatic nerve of a diabetic rat showing few degenerated myelinated nerve fibers with vacuolization in myelin sheaths forming fermentation chambers (asterisks). Electron-dense inclusions are detected in the axoplasm of myelinated (straight arrows) and unmyelinated axons (thick arrows). Retraction of the axoplasm of a myelinated nerve axon is noted (wavy arrow) with accumulation of periaxonal edema (O). The epineurium (E) is thickened with abundant collagen fibers (C) and subepineurial edema (So) is noted. **(TEM X 2500)**

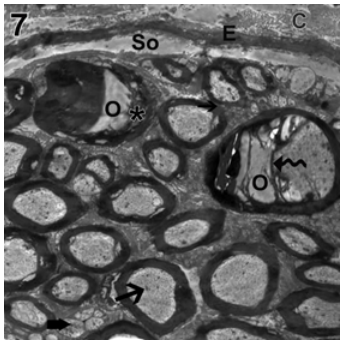

Vacuolation in myelin sheaths was evident (Figs. 7 & 9). Few fibers were enclosed by Schwann cells (Fig. 8). The axoplasm appeared pathologically affected. It was retracted with accumulation of periaxonal edema (Figs. 7 & 8). It exhibited electron-dense inclusions (Figs. 7 & 9).

Fig. 8: An electron micrograph of the sciatic nerve of a diabetic rat showing axonal retraction (wavy arrow) and periaxonal edema (O) in some fibers, one of which is enclosed by a Schwann cell (S). Epineurium (E) is thickened with splitting (Sp). **(TEM X 3000)**

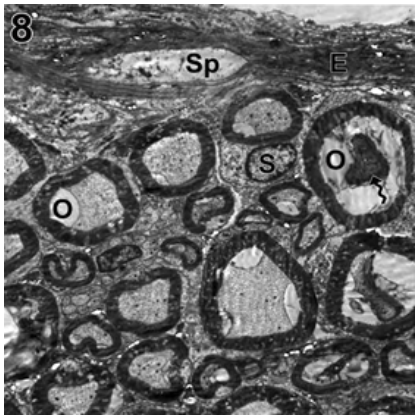

Macrophages were detected engulfing the myelin debris (Fig. 9). Electron-dense inclusions was found in the unmyelinated fibers as well (Fig. 7). The epineurium appeared thickened (Figs. 7 & 8) and showed partial splitting at discrete points along its length (Fig. 8) with focal sub-epineurial edema (Fig. 7).

Fig. 9: An electron micrograph of the sciatic nerve of a diabetic rat showing focal lysis (arrow heads) and vacuolizations (V) of the myelin sheath of some fibers. A macrophage (Mc) can be seen engulfing the myelin debris (My). Electron-dense inclusions (straight arrows) are detected in the axoplasm of the myelinated axons. **(TEM X 5000)**

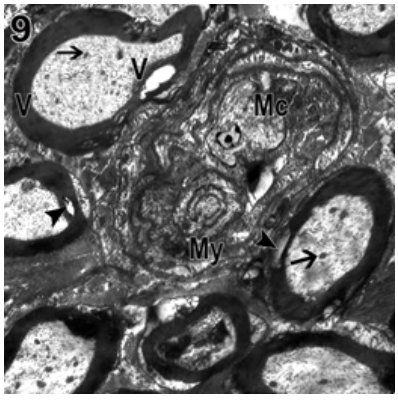

Ultrastructural examination of nerve sections of diabetic rats treated with *ClV* showed fewer morphological alterations, compared with those from non-protected diabetic rats. Myelin breakdown was significantly diminished and the ultrastructural features of axons showed minimal degenerative changes. Vacuolation and lamellar separation of myelin were less obvious. Further, the fine structure of Schwann cells appeared normal. No vacuoles were detected in the axoplasm of unmyelinated fibers and they seemed to be normal (Fig. 10).

Fig. 10: An electron micrograph of the sciatic nerve of a diabetic rat protected by CL V showing well-compacted myelin (My) in most of the nerve fibers. However, few fibers present vacuolated myelin sheath (asterisks). The axoplasm is well formed except small areas of minimal retraction (straight arrows). The unmyelinated axons (Um) and Schwann cells (S) appear with nearly normal ultrastructural configuration. **(TEM X 5000)**

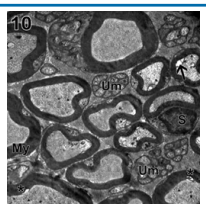

Qualitative Morphometric Results:
In semi thin sections, the control sciatic nerves (group I) consisted of 1–3 fascicles, and had a mean cross-sectional area of 74,425 µm2 [± 4916] (Table 3, Fig. 11). They enclosed a mean number of 7511 ± 452 myelinated nerve fibers (Table 3) of which 7313 ± 423 had a normal appearance [97.36 %] while 198 ± 40 appeared abnormal [2.64 %] (Table 3, Fig. 12).

Diabetic semithin sections (group III) presented a higher mean cross-sectional area of 95,691 µm2 ±5682 which was statistically significant compared to control group [P<0.05] (Table 3, Fig. 11). The myelinated nerve fibers had a mean number of 6308 ±431 with a statistically significant decrease (P<0.05) in the number of normally appearing myelinated nerve fibers compared to the control group to become 5677 ±385. On the other hand, the mean number of abnormally appearing myelinated nerve fibers significantly increased (P<0.05) compared to control group to become 632 ±49 (Table 3, Fig. 12). Abnormal appearance of myelinated nerve fibers included swelling, disrupted axoplasm and presence of myelin fragments.

Concomitant administration of CL V with Diabetes Mellitus (group IV) significantly decreased (P<0.05) the mean cross-sectional area of sciatic nerve to 86,486 µm2 [±4938] compared to Diabetic group (Table 3, Fig. 11). The myelinated nerve fibers had a mean number of 7373 [±447] with a statistically significant increase (P<0.05) in the mean number of normally appearing myelinated nerve fibers to become 6977 ±441, while the mean number of abnormally appearing myelinated nerve fibers significantly decreased (P<0.05) compared to the diabetic group to become 397 ±77 (Table 3, Fig. 12).

Table (3): Mean values (±S.D.) of cross-sectional areas, total number of axons, number (and percentage) of normally appearing myelinated axons and number (and percentage) of abnormally appearing myelinated axons in the entire sciatic nerve among the different groups

Group	Cross-sectional area of entire nerve (mean ±S.D.)	Total No. of Axons in the entire nerve (Mean ±S.D.)	No. of normally appearing myelinated axons (Mean ±S.D.)	Percent	No. of abnormally appearing myelinated axons (Mean ±S.D.)	Percent
Control	74,425 ± 4916	7511 ± 452	7313 ± 423	97.36 %	198 ± 40	2.64 %
DM	95,691 ± 5682	6308 ± 431	5677 ± 385	89.99 %	632 ± 49	10.01 %
DM + CL V	86,486 ± 5270*	7373 ± 447	6977 ± 441*	94.62 %	397 ± 77*	5.38 %

Significant compared to control group (P<0.05)
* Significant compared to Diabetic non treated group (P<0.05)

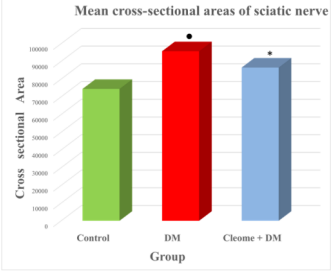

Fig. (11): Comparison between the mean values of cross-sectional areas of the entire sciatic nerve among the different groups

Significant compared to control group (P<0.05)
* Significant compared to diabetic non treated group (P<0.05)

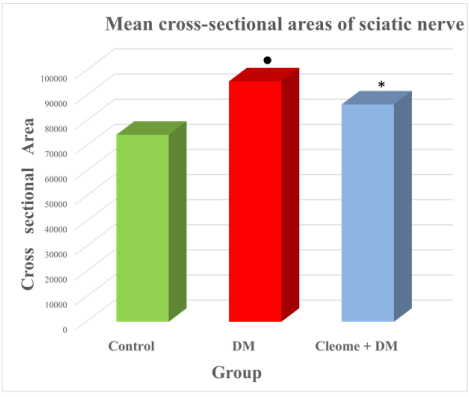

Fig. (12): comparison between percentages of normally appearing myelinated axons and abnormally appearing myelinated axons in the entire sciatic nerve among groups

Significant compared to control group (P<0.05)
* Significant compared to diabetic non- treated group (P<0.05)
DM: Diabetes mellitus

Discussion
DPN is one of the most common chronic complications of T2DM. About 50% of the population with T2DM will experience damage to the peripheral nerves at one stage of the disease. As these defects affect the quality of life, treatment of diabetic neuropathy or prevention of its accompanying symptoms has been considered a major goal **(Mehra et al., 2014).** The mechanism of the development of DPN has not yet been fully elucidated. Studies have shown that inflammatory reaction may play a role in the development of DPN **(Satoh et al., 2003).**

DPN comprises functional and structural changes in the peripheral nerves. Some of the morphological alterations in the myelinated fibers of the peripheral nerves associated with hyperglycemia were also seen in rat models of STZ-induced diabetic neuropathy **(Veiga et al., 2006).**

In the current work, DM- induced by STZ manifested by a significant increase in serum glucose concentration, compared with the control group. Diabetic rats also presented a significant decrease in body weight relative to controls. These findings were explained by **Morley et al. (2006).** They reported that elevated glucose level and diminished insulin level in DM trigger the release of triglycerides from adipose tissue and catabolism of amino acids in muscular tissue. This results in a loss of both fat and lean mass, leading to a significant reduction in total body weight.

At the morphological level, neuropathy was evident in the rats of the DM group in the current study by focal damage to myelinated fibers. This multifocal lesion, suggested an ischemic etiology **(Dyck et al., 1986a; Dyck et al., 1986b).**

The pathological lesions detected in the present work ranged from axonal atrophy, axonal shrinkage and axon–myelin separation up to total axonal destruction and loss. Myelin sheath revealed vacuolization with the formation of fermentation chambers. It was previously hypothesized that axonal shrinkage and separation from the myelin sheath and peri-axonal edema could explain the marked degenerative changes in the nerve fibers with consequent reduction in nerve conduction of STZ models **(Brussee et al., 2006).**

Axonal shrinkage, myelin separation, vacuolization and disorganization was reported by **Chen et al., (2016)** in experimental diabetic rats. They attributed these morphological

changes to Diabetes and hyperglycemia. Hyperglycemia also led to increased expression of E-selectin, and Intercellular Adhesion Molecule 1 (ICAM-1) by endothelial cells **(Wu et al., 2016).** Increased ICAM-1 expression in the endothelial cell surface attracted monocytes, neutrophils, and T lymphocytes and endothelial cells, resulting in direct endothelial cell injury by proteases and oxygen free radical release **(Wang et al., 2015).** Previous studies have found that blocking ICAM-1 can prevent leukocytosis as well as retinal vascular leakage **(Kaseb et al., 2007).**

In the present study, severe demyelination was detected with evidence of myelin destruction in the form of splitting and decompaction of myelin lamellae. Vacuolization of myelin sheaths was evident with formation of fermentation chambers. Honeycomb degeneration of myelin was seen. This was previously described by other investigators as grade 3 degeneration of myelin comprising separation of myelin and disruption of myelin configuration **(Vargel, 2009).**

As in any neuropathy, macrophages engulfing the myelin debris were observed in the current work. Role of inflammation in neuropathy was previously described by **(Mingdi et al., 2015).** They described the role of anti-inflammatory agents in protection against DPN. Loss of salutatory conduction of nerve impulses that results from demyelination leads to decrease in conduction velocity and conduction block **(Sharma et al., 2002).**

Onion-bulb formation with layers of Schwann cell processes enwrapping the axon was evident in the diabetic unprotected group in the current work. Onion bulbs are concentric lamellar structures formed by Schwann cell processes, which may be seen in several generalized or localized diseases of the peripheral nerve, including diabetic neuropathy **(La Point et al., 2000).** A large number of studies demonstrated that Schwann cells are closely implicated in the pathogenesis of diabetic peripheral neuropathy **(Coste et al., 2004).** Schwann cell abnormalities may cause nerve dysfunction, such as reduced nerve conduction velocity, axonal atrophy and impaired axonal regeneration. Proliferation of Schwann cells was inhibited by high concentrations of glucose (**Chen et al., 2016).**

The epineurium appeared thickened and irregular with subepineurial edema in the present study. This edema was previously described by **(Mingdi et al., 2015).** Edema observed in the current work probably played a role in reducing the endoneurial blood flow. Consequently, it can be largely responsible for the degenerative changes in Schwann cells and myelinated nerve axons described in the present study. It could also be an important factor in the pathogenesis of neuropathy in diabetic rats, which supported the conclusions of other studies that considered ischemia to be characteristic of hyperglycemic models **(Cameron et al., 1991).**

In the current work, neurofilaments and electrondense inclusions accumulated in the axoplasm of most degenerating axons, probably because of stagnation of axoplasmic flow. These dense inclusions were previously described by other authors who postulated that tissue lysosomal phospholipid content increased in DM, forming intralysosomal inclusion bodies that were indigestible by phospholipases **(Coste et al., 2004).** Later events in diabetic neuropathy may interpret the impaired axonal transport of neurofilaments or other cytoskeletal structures. Limited cytoskeletal support by perikarya may result in flawed axons or axons that are incapable of dynamic restructuring, probably resulting from rapid glycosylation of proteins **(Kennedy and Zochodne, 2005).**

Degenerative nerve changes reported in the current work were proved by morphometric statistical analysis. Diabetic semithin sections presented a higher mean cross-sectional area of 95,691 μm^2 ±5682 which was statistically significant compared to control group [P<0.05]. This may be attributable to an inflammatory process with edema and fluid accumulation. The myelinated nerve fibers had a mean number of 6308 ±431 with a statistically significant decrease (P<0.05) in the number of normally appearing myelinated nerve fibers compared to the control group to become 5677 ±385. On the other hand, the mean number of abnormally appearing myelinated nerve fibers significantly increased (P<0.05) compared to control group to become 632 ±49.

Decrease in nerve blood flow in diabetic neuropathy could lead to nerve metabolic abnormality and consequently to defects in ATP-sensitive ion exchanger pumps like the Na–K pump. Defects in the Na–K pump could finally lead to membrane inability to preserve the resting potential and consequent disturbance in nerve conductivity **(Moretti et al., 2009).**

Different mechanisms for the pathogenesis of diabetic complications have been described but none has achieved general acceptance. These mechanisms have been divided into two major categories: the first was a metabolic etiology and the second was a vascular etiology **(Fazan et al., 2010).** The formation of advanced glycation end products may explain many of the diabetic complications. In terms of DPN, the protein glycation cascade might lead either to demyelination or to axonal atrophy. Glycation of the myelin proteins would account for myelin destruction and consequent demyelination. In contrast, glycation of collagen could lead to a reduction in nerve growth factor, leading to axonal atrophy **(Harati, 2007).**

Moreover, diabetic neuropathy had been attributed to accumulation of reactive oxygen species (ROS), especially superoxide radicals, and hydrogen peroxide release **(Lu et al., 2010).** Oxidative stress results from an imbalance between radical-generating and radical scavenging systems – that is, increased free radical production or reduced activity of antioxidant defenses or both. As oxidative stress plays an important role in the development of complications in DM, potent antioxidants are now being investigated. Antioxidant therapy has been thought to decrease oxidative stress **(Rösen et al., 2001).**

The vascular theory assumes that hyperglycemia and metabolic derangement affect the structure and function of endoneurial micro vessels, which then induce fiber changes by altering the blood–nerve barrier, inducing hypoxia or ischemia **(Turkoglu et al., 2012).**

Ultrastructural examination of nerve sections of diabetic rats treated with Cl V in the current study showed fewer morphological alterations, compared with those from non-protected diabetic rats. Myelin breakdown was significantly diminished and the ultrastructural features of axons showed minimal degenerative changes. Vacuolation and lamellar separation of myelin were less obvious. Further, the fine structure of Schwann cells appeared normal. No vacuoles were detected in the axoplasm of unmyelinated fibers and they seemed to be normal. Moreover, concomitant administration of CL V with Diabetes Mellitus significantly decreased (P<0.05) the mean cross-sectional area of sciatic nerve to 86,486 μm^2 [±4938] compared to Diabetic group. The myelinated nerve fibers had a mean number of 7373 [±447] with a statistically significant increase (P<0.05) in the mean number of normally appearing myelinated nerve fibers to become 6977 ±441, while the mean number of abnormally appearing myelinated nerve fibers significantly decreased (P<0.05) compared to the diabetic group to become 397 ±77.

The protective effect of Cl V may be attributed to its antioxidant effect (**Jayaprakash et al., 2016).** They studied the anti-oxidant, cytotoxic and anticancer properties of Cl V extract. They screened carbohydrates, glycosides, flavonoids, phytosterols and triterpenoids in the plant. **Pillai and Nair (2015)** evaluated the reactive oxygen species (ROS) scavenging and in vitro antioxidant activities of Cl V. They used different assays such as the 2,2-diphenyl-1-picrylhydrazyl (DPPH), ferric reduction activity potential (FRAP) and 2,2-azino-bis-3-ethylbenzothiazoline-6-sulfonic acid (ABTS) methods for hydroxyl, superoxide, nitric oxide, and hydrogen peroxide free radicles. The extract gave positive results with all assays used.

Conclusion: Diabetic neuropathy was evident in the rat models four weeks after induction of DM by STZ. Morphological abnormalities targeted the nerve fibers, myelin sheath, and Schwann cells. CL V administration before DM induction, reduced the neuro-destructive process of DM and yielded neuroprotection against damages resulting from the diabetic state. This neuroprotective effect of CL V could be attributable to its antioxidant, anti-inflammatory properties in addition to its hypoglycemic effect. The beneficial effects of the antioxidant treatment supported the hypothesis that oxidative stress and free radicals played a principal role in neuronal pathology in DM.

Recommendations: Individuals who are considered to be at high risk for development of DM, especially when DM runs in families, should be identified. Diabetic outpatient clinics should be screened for the prevalence of PN. In view of our findings on experimental rats, CL V is recommended as a promising agent for the prevention of diabetic neuropathy in newly diagnosed diabetic patients, provided that future human studies also prove similar neuroprotective effects of CL V. Further molecular research is needed to elucidate the precise mechanism of action and examine the potential therapeutic effects of CL V on diabetic tissue damage, particularly in humans.

Acknowledgement
The authors would like to express their sincere gratitude to the deanship of scientific research, University of Tabuk, for generously funding this work.

REFERENCES

1. Agrawal N K, Kant S. Targeting inflammation in diabetes: Newer therapeutic options. World J Diabetes, 2014; 5, 697–710.
2. Alamoudi O S, Attar S M, Ghabrah T M, Al-Qassimi M A. Pattern of common diseases in hospitalized patients at an University hospital in Saudi Arabia; A Study of 5594 Patients. Journal of King Abdulaziz University: Med. Sci., 2009; 16 (4): 3-12.
3. Alqurashi K A, Aljabri K S, Bokhari S A. Prevalence of diabetes mellitus in a Saudi community. Ann Saudi Med., 2011; Jan-Feb; 31(1): 19–23.
4. Armitage P, Berry G. Medical research. Statistical methods. In: Armitage P, Berry G, editors. Medical research. 3rd ed. London: Blackwell Scientific Publications, 1994; 12–48.
5. Boddapati S R, Kasala E R, Kumar P, Bodduluru L N, Sriram C S, Lahkar M. Effects of Cleome viscosa on hyperalgesia, oxidative stress and lipid profile in STZ induced diabetic neuropathy in Wistar rats. Pak. J. Pharm. Sci., 2014; 27(5), 1137-1145.
6. Bose U, Bala V, Ghosh TN, Gunasekaran K, Rahman AA. Antinociceptive, cytotoxic and antibacterial activities of Cleome viscosa leaves. Rev. bras. farmacogn. Braz J of Pharmacognosy, 2011; 21(1): 165-169. doi: 10.1590/S0102-695X2011005000023.
7. Boyina Chaya D, Chakrapani R. Studies on anti-diabetic activity of Cleome viscosa in alloxan-induced diabetic rats. South American Journal of Academic Research, 2015; 2, (1): 1-8.
8. Brussee V, Guo G, Dong Y, Cheng C, Martinez J A, Smith D, et al. Distal degenerative sensory neuropathy in a long-term type 2 diabetes rat model. Diabetes, 2008; 57:1664–1673.
9. Callaghan B C, Little A A, Feldman E L, Hughes R A. Enhanced glucose control for preventing and treating diabetic neuropathy. Cochrane Database Syst., 2012; Rev. 6: CD007543.
10. Cameron NE, Cotter MA, Low PA. Nerve blood flow in early experimental diabetes in rats: relation to conduction deficits. Am J Physiol 1991; 261:E1–E8.
11. Chan L, Terashima T, Urabe H, Lin F, Kojima H. Pathogenesis of diabetic neuropathy: bad to the bone. Ann N Y Acad Sci., 2011; 1240, 70–76.
12. Chen L, Li B, Chen B, Shao Y, Luo Q, Shi X, Chen Y. Thymoquinone Alleviates the Experimental Diabetic Peripheral Neuropathy by Modulation of Inflammation. Sci Rep., 2016; 22; 6:31656. doi: 10.1038/srep31656.
13. Coste TC, Gerbi A, Vague P, Maixent JM, Pieroni G, Raccah D. Peripheral diabetic neuropathy and polyunsaturated fatty acid supplementations: natural sources or biotechnological needs? Cell Mol Biol (Noisy-le-grand) 2004; 50:845–853.
14. Das A, Mukhopadhyay S. The evil axis of obesity, inflammation and type-2 diabetes. Endocr Metab Immune Disord Drug Targets, 2011; 11, 23–31.
15. Dyck P J, Karnes J L, O'Brien M S, Okazaki L, Engelstad J. The spatial distribution of fiber loss in diabetic polyneuropathy suggests ischemia. Annals of Neurology, 1986a; 19 (5): 440–449.
16. Dyck P J, Lais A, Karnes J L, O'Brien P, Rizza, R. Fiber loss is primary and multifocal in sural nerves in diabetic polyneuropathy. Annals of Neurology, 1986b; 19 (5): 425–439.
17. Ewing D J, Campbell I W, Clarke B F. Mortality in diabetic autonomic neuropathy. Lancet, 1976; 1, 601–603.
18. Farmer K L, Li C and Dobrowsky R T. Diabetic peripheral neuropathy: should a chaperone accompany our therapeutic approach? Pharmacol Rev., 2012; 64, 880–900.
19. Fazan VPS, de Vasconcelos CAC, Valença MM, Nessler R, Moore KC. Diabetic peripheral neuropathies: a morphometric overview. Int J Morphol 2010; 28:51–64.
20. Fox C S, Coady S, Sorlie P D, Levy D, Meigs J B, D'Agostino R B Sr, et al. Trends in cardiovascular complications of diabetes. J Am Med Assoc., 2004; 292:2495–2499.
21. Golbidi S, Ebadi S A, Laher I. Antioxidants in the treatment of diabetes. Curr Diabetes Rev., 2011; 7:106–125.
22. Guariguata L, Whiting D R, Hambleton I, Beagley J, Linnenkamp U, Shaw J E. Global estimates of diabetes prevalence for 2013 and projections for 2035. Diabetes Res Clin Pract., 2014; 103 (2), 137–149.
23. Gürpinar T, Ekerbiçer N, Uysal N, Barut T, Tarakçi F, Tuglu M I. The effects of the melatonin treatment on the oxidative stress and apoptosis in diabetic eye and brain. Scientific World J., 2012; 498489.
24. Harati Y. Diabetic neuropathies: unanswered questions. Neurol Clin., 2007; 25:303–317.
25. Hayat M A. Principals and techniques of electron microscopy: biological application. 4th ed. Edinburgh, UK: Cambridge University Press, 2000; 37–59.
26. Inserra M M, Yao M, Murray R, Terris D J. Peripheral nerve regeneration in interleukin 6-deficient mice. Arch Otolaryngol Head Neck Surg., 2000; 126: 1112-1116.
27. Jana A, Biswas S M. Lactam nonanic acid, a new substance from Cleome viscosa with allelopathic and antimicrobial properties. Journal of Biosciences, 2011; 36(1): 27-35.
28. AP J, Krishnakumar KR, Srinivasan KK, Harindran J, Mohammed SP. Evaluation of antioxidant, cytotoxic and anticancer effects of Cleome Viscosa Linn. European journal of pharmaceutical and medical research, 2016; 3(4): 253-262.
29. Kaseb, A.O., Chinnakannu, K., Chen, D., Sivanandam, A., Tejwani, S., Menon, M., Dou, Q.P. and Reddy, G.P.V. Androgen receptor and E2F-1 targeted thymoquinone therapy for hormone-refractory prostate cancer. Cancer Res., 2007; 67, 7782–7788.
30. Kawada N, Moriyama T, Kitamura H, Yamamoto R, Furumatsu Y, Matsui I, Takabatake Y, Nagasawa Y, Imai E, Wilcox C S, Rakugi H, Isaka Y. Towards developing new strategies to reduce the adverse side-effects of nonsteroidal anti-inflammatory drugs. Clin Exp Nephrol., 2012; 16 (1), 25–29.
31. Kennedy JM, Zochodne DW. Experimental diabetic neuropathy with spontaneous recovery: is there irreparable damage? Diabetes 2005; 54:830–837.
32. Kissin I, Freitas CF, Mulhern HL and DeGirolami U. Sciatic nerve block with resiniferatoxin: an electron microscopic study of unmyelinated fibers in the rat. Anesth Analg., 2007; 105(3):825-831.
33. LaPoint SF, Powers JM, Woodruff JM, MacCollin M, Jacoby LB, Vortmeyer AO, et al. Schwann cell-onion bulb tumor of the trigeminal nerve: hyperplasia, dysplasia or neoplasia? Acta Neuropathol., 2000; 99:67–72.
34. Lenzen, S. (2008): The mechanisms of alloxan- and streptozotocin-induced diabetes. Diabetologia; 51:216–226.
35. Lu, J., Wu, D.M., Hu, B., Cheng, W., Zheng, Y.L., Zhang, Z.F., Ye, Q., Fan, S.H., Shan, Q. and Wang, Y.J. Chronic administration of troxerutin protects mouse brain against d-galactose-induced impairment of cholinergic system. Neurobiol Learn Mem 2010; 93:157–164.
36. Mehra M, Merchant S, Gupta S, Potluri, R. C. Diabetic peripheral neuropathy: resource utilization and burden of illness. J Med Econ., 2014; 17, 637–645.
37. Mingdi L, Da H, Xiaoxing L, Lan L, Tang-Tong-Fang Confers Protection against Experimental Diabetic Peripheral Neuropathy by Reducing Inflammation. Evidence-Based Complementary and Alternative Medicine. Volume 2015 (2015), Article ID 574169, 12 pages http://dx.doi.org/10.1155/2015/574169
38. Moretti B, Notarnicola A, Maggio G, Moretti L, Pascone M, Tafuri S, Patella V. The Bmanagement of neuropathic ulcers of the foot in diabetes by shock wave therapy. BMC Musculoskeletal Disord., 2009; 10:54.
39. Morley J E, Thomas D R, Wilson M-MG. Cachexia: pathophysiology and clinical relevance. Am J Clin Nutr., 2006; 83:735 - 743.
40. Pillai LS, Nair BR. Radical scavenging potential of cleome viscosa L. and cleome burmanni W. & A. (cleomaceae). International journal of pharmaceutical sciences and research, 2013; 4 (2): 698-705.
41. Rösen P, Nawroth PP, King G, Möller W, Tritschler H-J, Packer L. The role of oxidative stress in the onset and progression of diabetes and its complications: a summary of a congress series sponsored by UNESCO-MCBN, the American Diabetes Association and the German Diabetes Society. Diabetes Metab Res Rev 2001; 17:189–212.
42. Satoh J, Yagihashi S, Toyota T. The possible role of tumor necrosis factor-alpha in diabetic polyneuropathy. Exp Diabesity Res., 2003; 4, 65–71.
43. Sharma KR, Cross J, Farronay O, Ayyar DR, Shebert RT, Bradley WG. Demyelinating neuropathy in diabetes mellitus. Arch Neurol 2002; 59:758–765.
44. Tesfaye S, Selvarajah D. Advances in the epidemiology, pathogenesis and management of diabetic peripheral neuropathy. Diabetes Metab Res Rev., 2012; 28 Suppl 1, 8–14.
45. Turkoglu, E., Serbes, G., Dolgun, H., Oztuna, S., Bagdatoglu, O.T., Yilmaz, N., Bagdatoglu, C. and Sekerci, Z. Effects of -MSH on ischemia/reperfusion injury in the rat sciatic nerve. Surg Neurol Int 2012; 3: 98501.
46. Vargel I. Impact of vascularization type on peripheral nerve microstructure. J Reconstr Microsurg 2009; 25:243–253.
47. Veiga S, Leonelli E, Beelke M, Garcia-Segura L M, Melcangi R C. Neuroactive steroids prevent peripheral myelin alterations induced by diabetes. Neurosci Lett., 2006; 402:150–153.
48. Vileikyte, L., Peyrot, M., Bundy, C., Rubin, R.R., Leventhal, H., Mora, P., Shaw, J.E., Baker, P. and Boulton, A.J. The development and validation of a neuropathy- and foot ulcer-specific quality of life instrument. Diabetes Care., 2003; 26, 2549–2555.
49. Wang X, Shi L, Han Z, Liu B. Follistatin-like 3 suppresses cell proliferation and fibronectin expression via p38MAPK pathway in rat mesangial cells cultured under high glucose. Int J Clin Exp Med., 2015; 8, 15214–15221.
50. Wu, J.H., Wang, Y.H., Wang, W., Shen, W., Sang, Y.Z., Liu, L. and Chen, C.M. MiR-18b suppresses high-glucose-induced proliferation in HRECs by targeting IGF-1/IGF1R signaling pathways. Int J Biochem Cell Biol., 2016; 73, 41–52.
51. Wu K K and Huan Y. Streptozotocin-induced diabetic models in mice and rats. Curr Protoc Pharmacol., 2008; (Suppl 40):5.47.1–5.47.14.
52. Yasuda, H., Terada, M., Maeda, K., Kogawa, S., Sanada, M., Haneda, M., Kashiwagi, A. and Kikkawa, R.. Diabetic neuropathy and nerve regeneration. Prog Neurobiol, 2003; 69, 229–285.